

We are IntechOpen, the world's leading publisher of Open Access books Built by scientists, for scientists

6,900

Open access books available

186,000

International authors and editors

200M

Downloads

Our authors are among the

154

Countries delivered to

TOP 1%

most cited scientists

12.2%

Contributors from top 500 universities



WEB OF SCIENCE™

Selection of our books indexed in the Book Citation Index
in Web of Science™ Core Collection (BKCI)

Interested in publishing with us?
Contact book.department@intechopen.com

Numbers displayed above are based on latest data collected.
For more information visit www.intechopen.com



Inertial Navigation Systems and Its Practical Applications

Aleksander Nawrat, Karol Jędrasiak, Krzysztof Daniec and Roman Koteras

Additional information is available at the end of the chapter

<http://dx.doi.org/10.5772/50578>

1. Introduction

Nowadays one of the most common problems for science is the answer for the question how to improve our tools. Each year there are more attempts to solve the problem. Designed and created tools and prototypes' capabilities are increasing each year. In XXI century there is a trend to design tools that require as little human interaction as possible to fulfill their tasks.

Main intention of autonomous devices' designers is to develop tools used for implementation tasks, such as unknown territory exploration or performing tasks in strong radiation fields which are dangerous for human health and life. Unmanned flying objects used for military, mobile robots, space ships, exoskeletons or intelligent clothing monitoring body signals. These are only a few examples of useful devices that are being developed at the moment.

One of the main problems during autonomous mobile objects' development is the problem of precise navigation. In order to navigate the object it is required to know the exact position and orientation of the object in relation to the known environment. Creation of a sensor system capable of an environment perception as well as monitoring inner object parameters is an important problem in the unmanned mobile objects field. Control algorithms are designed on the top of available sensor data, therefore their flexibility and reliability are common requirements.

Recently, there is a lot of research being performed in the area of inertial measuring object orientation. Inertial measurement units (IMUs) are electronic devices used for detection of the current object orientation. Usually they measure changes in object's rotation and acceleration. As a measurement devices, they must fulfill a set of requirements e.g. smallest possible size and weight, configurable filtered output data. Sensor should be capable of working in the extreme temperature and pressure conditions. The main requirement is to

deliver high quality data with the highest speed possible. For mobile devices there is also an additional requirement of minimal electrical energy consumption.

In order to fulfill mentioned requirements, modern inertial measurement units are utilizing the newest technology achievements. Such sensors usually consist of at least two different types of subsensors. First type is an accelerometer measuring linear acceleration. Second is a gyroscope measuring angular acceleration value. Additionally, there are also different types of sensors mounted inside of IMU. One of the most popular additional sensors are reference magnetometers used for detection of north direction. Other types are temperature sensors used for temperature compensations algorithms and in case of UAV - altimeters.

Linear accelerometers measure object's linear acceleration and therefore detect direction of object's movement. In order to measure movement regardless of autonomous device's type there are usually three measurement axes X, Y and Z (fig. 1). For each axis there is a separate linear accelerometer. Modern sensors allow to measure data along all three axes by a single chip. Accelerometers are for instance used for collision detection, object's orientation measurement or as user interface. There are various methods of measuring linear acceleration. Due to this reason, there are sensors using capacity, piezoelectric, piezoresistant, magneto responsive, based on Hall effect and microelectromechanical systems (MEMS).

Gyroscopes are sensors which also measure acceleration. However it is not linear acceleration but angular. There are also three axes of measurement. They are traditionally called yaw, pitch and roll. Axes coordinate system are shown in fig.1. Gyroscopes are based on the law of conservation of momentum. In order to operate, they are required to preserve high rotation speed on the one side low and friction in bearings on the other side. There are three main types of gyroscopes: mechanical, optical and MEMS. Mechanical and optical sensors are much larger than MEMS, therefore the latter are usually used in practical solutions.

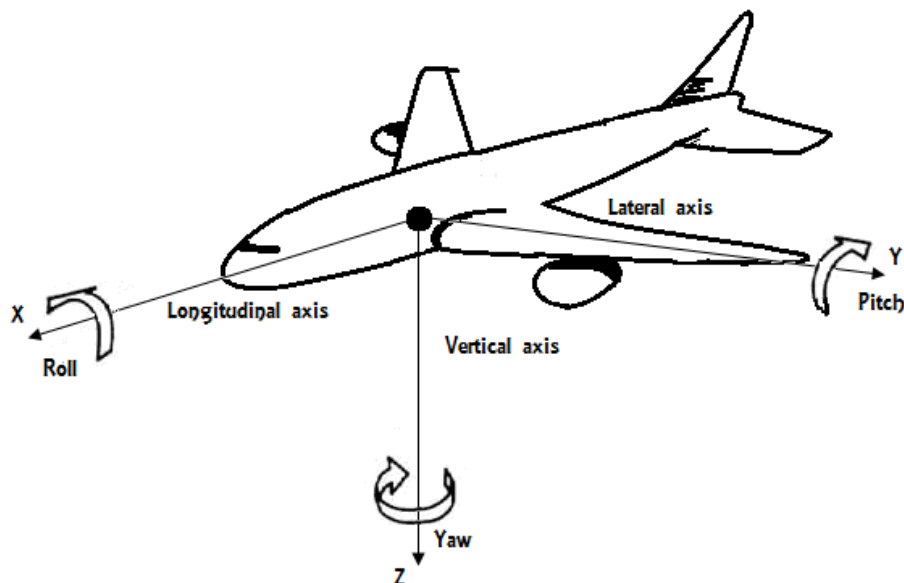


Figure 1. Three measurement axes for IMU.

Recently, most of the manufactured inertial measurement units are based on MEMS technology. Regardless of easy usability, the main advantage of such devices is considerably its small size. Electromicromechanical chips are made of silicon, glass and polymer materials. Masks for processors are made using microelectrical technologies as e.g. photolithography. MEMS sensors' circuits are divided into two parts. The first, mechanical part is responsible for measuring angular and linear velocity. The electronic part using analog-digital converter converts signals from the mechanical part. Because of relatively large surface to volume ratio there are dominating electrostatic phenomenon over the mass inertia.

Micromechanical systems are commonly used in navigation of mobile platforms and vehicles, for autopilots of aerial ships, boats or ground units. Another use is in aiding stabilization of opto-electrical gimbals. The IMUs are also used for seatbelts locking during detected crash moment, in PCs for HDD security during fall. It is also used in photo cameras for elimination of vibration effects. Modern toys for children also utilize inertial measurement units.

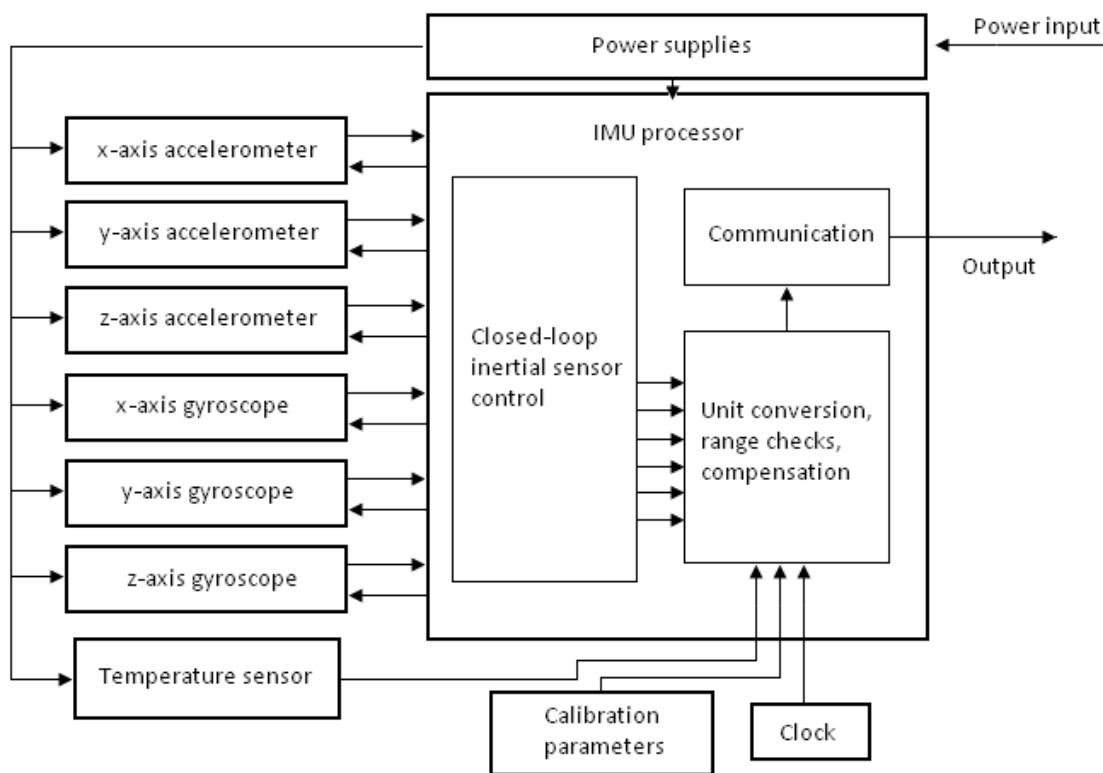


Figure 2. Inertial measurement unit operations schema.

An example of IMU working schema is presented in fig.2. Linear (x, y, z) and angular (f_x , f_y , f_z) acceleration information is enough to estimate objects speed and further their position in space. Exemplary IMU is a 6-DOF type, which means it can measure signals in six dimensions. Raw data from sensors is converted to the known sensor's shell coordinate system. Measure values are converted to the respective physical units. Required parameters for transformation are computed during calibration phase of the sensor. It is useful to relate coordination systems to external, known reference coordinate system. Such reference

coordinate system might be magnetic field of the Earth. Using magnetometers it is possible to measure the magnet response and after taking into account magnetic deviations depending on the current latitude and longitude, it is possible to estimate the north direction. Inertial measurement units also using magnetometers are called 9-DOF IMU.

IMUs internal processing frequency can be as high as 500 Hz. However output data rate is usually in range between 80 and 100 Hz.

Inertial measurement units are unfortunately subjects of a bias error. However, those errors can be measured in laboratories and computed fixes are stored in devices' flash memory. Sensor readings are also affected by the temperature of environment. Therefore each IMU is calibrated in climate chamber for full temperature operating range in order to establish compensation parameters. For temperature compensation installation of additional temperature sensor is required.

An affair of a great importance is devices' miniaturization. Nowadays, more and more research is being conducted all over the world in order to make current sensors smaller and lighter. Such miniaturized sensors could be used in micro military or medical robots. Micro-robots require smaller mechanical and propulsion parts. Size reduction is still a challenging task for scientists. It is essential for UAVs to reduce the total weight of mounted sensors. Possible applications of micro-sensors are tiny helicopters invisible for radars or capable of flying not only outdoors but also indoors. There is also a wide area for practical medical implementations. Recently, there is a lot of interest in the field of rehabilitation exoskeletons. Exoskeletons are electro-mechanical devices amplifying patients muscles' effective power. They are controlled by natural micro-electric signals in muscles measured by electromyography. For such devices it is important to deliver reliable data from precisely chosen anthropomorphic points. Significantly reduced size of the sensor would allow to reduce the impact on the patient during acquisition. Therefore, measured movements would be closer to the natural patient's movement. Acceptable volume of such micro sensors should be around 2cm³ in order to not affect person's natural movements. Micro IMUs of a size not affecting movements could be used as a part of intelligent clothing. Knowledge about human's body parts' orientation would allow clothing to accommodate to person position. For instance, intelligent soldier uniform could enable masking mode every time the soldier starts crawling. Another implementation could monitor patients movements in order to detect e.g. Parkinson disease effects or measure pulse during everyday actions. It could be used as a tool for detection elderly people's potential threats in home environment.

2. Navigation aids

Navigation using only inertial measurement units is difficult or even impossible due to the accumulative character of possible errors. Typical errors of accelerometers and gyroscopes are biases, scale factors, triad non-orthogonalities and noise. Bias is defined as an independent and uncorrelated of the specific force and angular velocity experienced by the unit. The bias value affecting the unit consists usually of two or more sources of bias. The turn on bias commonly contains about 90% of the bias. Standard and temperature bias

impact is estimated at about 10%. However the temperature bias in the MEMS IMU's can have similar magnitude as the turn on bias. A scale factor error is a ratio of change in the output of the sensor with respect to true intended measurement. It can be estimated by the filter implemented in the inertial measurement unit. Another type of error is cross coupling errors which is the result from the non-orthogonality of the sensor triad. The error is estimated during the calibration and the required corrections are applied before using the sensor. Another type of error is existing within the gyroscopes which work due to use a spinning or vibratory mass. The source of the error is imbalance in the proof mass and the magnitude varies in the range from 1 to 100°/hr/g. It implies that units which are subjected to an acceleration of multiple [g] can be affected with an error of thousands of degrees per hour. The last type of error is a random noise error that comes from electrical and mechanical instabilities. It is known that during static operation the error follows Gaussian distribution however during unit movement the error distribution changes.

In order to aid the navigation the readings from the IMUs are compared against measurements from the independent sources. Various data fusion algorithms are used for combining the information from various external sources. One of the oldest of the still used navigation aids is using ground-based transmitting stations. Combination of bearings to at least two ground stations can be used to compute the exact position of the unit by a simple process of triangulation. In order to cover large areas it is desired to use low frequencies of electromagnetic waves. However the process of radio propagation is affected by the current condition of the atmosphere the readings may be unreliable. Hence, regardless the lower range higher frequencies are often used. Small corrections are always better than no corrections therefore a long-range navigation systems are also used. An example of such system is a Loran C system consisting of a master station and a chain of slave stations. The idea of operation of the system is measuring the time of arrival of the signal from the previous chain node. Using the time difference it computes the correction and broadcast it further to the next nodes and potential unit listeners.

It is well known that the stars may be used as a references for the purposes of celestial navigation. It is required to know the positions of at least two celestial objects in relation to the observer and the exact time of the observation. Knowledge of a position of a celestial object in relation to the observer allows to draw a circle centered on the point on the Earth directly below the observed object. There are pre-computed astronomical tables in which the center points of the circles can be found using the exact time of the measurement. It is assumed that an observer must be located at the circles intersection. Application of the following technique to the navigation using the INS requires development of an automatic measuring device. There are known such devices called star trackers however their accuracies are about three hundred meters on the surface of the Earth. Hence, such devices are rarely used in order to improve the quality of the INS.

Another type of a navigation aid is using a surface radar stations. It is possible to measure the line-of-sight from the ground station to the observed air ship. From the measurements the air ship vehicle's range (R), elevation, azimuth and bearing can be computed with respect to a local reference frame at the location of the radar ground station. The relative

position of the object in the air and a known ground position of the station can be transmitted to the air object in order to compute the corrections and aid the INS.

$$\begin{aligned} R &= \sqrt{x^2 + y^2 + z^2} \\ \psi &= \tan^{-1}\left(\frac{y}{x}\right) \\ \theta &= \tan^{-1}\left\{\frac{z}{\sqrt{x^2 + y^2}}\right\} \end{aligned} \quad (1)$$

Navigation aids can also be installed directly on the board of the unit e.g. air ship. One of such devices is a Doppler radar. It operates by transmitting a narrow beam of the microwave energy to the ground and measures the frequency shift that occurs in the reflected signal as a result of the relative motion between the aircraft and the ground. Let's assume that the air ship velocity is equal to V and the angle between the ground and the radar beam is θ , the frequency shift can be computed as:

$$\frac{2V}{\lambda} \cos\theta, \quad (2)$$

where λ is the wavelength of the radar beam used for the transmission. Usually it is in the frequency range 13.24 – 13.4 GHz which stands for $\lambda \approx 0.22$ dm. In order to estimate the velocity of an object capable of moving in three dimensions the number of radar beams used must be no smaller than three. Modern systems use a planar array of beams processed independently and computed by microprocessors.

Another navigation aid is based on measuring atmospheric pressure readings in order to estimate the height of the object. Altimeters due to their relatively high precision (typically less than 0.01 percent) are used to bound the growth of error in a vertical direction of the INS. The altimeter measurements can also be made by using sonic or ultra-sonic waves radar. Combination of height above ground and height above sea level values can be used in order to match a detailed map of a terrain. A sequence of such measurements accompanied by the orientation of the object from the INS can be fitted into the surface. However such application requires a map of terrain and that the air ship is moving above a terrain with a contour variation above 20%. It is difficult or impossible to use this technique over the sea. Recently laser rangefinders are becoming more and more popular in the field of measuring the distance however the technique is still limited to a short range over the ground.

Another technique possible to use as a navigation aid is a scene matching. A video camera mounted below the air ship delivers a sequence of images of the ground. If the scene visible in the ground can be recognized as a location with a known geographical coordinates it is possible to compute the corrections to the INS. The recognition is usually performed on the basis on two types of features. First are linear features detected in the image as edges and further extracted using techniques as Hough transform or active contours. Another type of features are SIFT like features consisting of a unique description of a point in the image that is scale, rotation, translation and illumination invariant. A combination of a terrain and a scene matching is map matching technique. First a geographical coordinates of a roads visible below are computed using scene recognition techniques. Next an air ship trajectory is

fitted to the matching roads and finally any errors are corrected by the assumption that the object is moving only within the roads net. A variation of map matching technique is commonly used in car and pedestrian navigations.

One of the most popular navigation aids is using a magnetometers. The devices capable of measuring the magnetic field of the Earth. Regardless the type of the magnetometer it is measuring the magnetic field in a one, two or three dimensions. Two most commonly used as a navigation aid are 3D magnetometers. Almost any metal device has its own magnetic field that cannot be distinguished from the field of Earth, therefore a calibration of the magnetometers after mounting is required. After calibration it could be used as an 3D electronic compass with measurements expressed in a local object frame. The relationship between the magnetometer readings (M_x, M_y, M_z) and object's attitude can be expressed as follows:

$$\begin{bmatrix} M_x \\ M_y \\ M_z \end{bmatrix} = C_n^b \begin{bmatrix} E \cos \delta \cos \gamma \\ E \cos \delta \sin \gamma \\ E \sin \delta \end{bmatrix}, \quad (3)$$

where C_n^b is a cosine matrix of the object with respect to the local geographic frame and E is the Earth's magnetic field. Magnetometers capability of measuring the magnetic field does not limit their usage only as an electronic compass. It is possible to measure local magnetic variation in the planet field. Such information could be stored in a map and used to navigate in a similar manner to terrain matching.

The most popular navigation aid is satellite navigation. Currently the most widely used system was names Global Positioning Systems Navigation Signal Timing And Ranging in short GPS. It consists of 31 satellites circling around the Earth. It is able to provide geographical location and time regardless the weather conditions nor the place on or near the Earth. In order to use the GPS information a GPS receiver is required. It listens for the information from the satellites. Each satellite transmits the time the message was transmitted and satellite position at the time of message transmission. Receiver using the acquired information computes by trilateration its distance to each satellite in the field of view. This distance is called pseudo-range. It is essential for very precise time measuring in the satellites because even small clock error is multiplied by the speed of light which results in a significant location miscalculations. A satellite's position and pseudo-range define a sphere, centered on the satellite with a radius equal to the pseudo-range. Therefore the position of the receiver is somewhere on the surface of the sphere. With at least four satellites the position of the GPS receiver should be at the intersection of the surfaces. However due to time measurement and atmospheric signal propagation errors the accuracy of the GPS is varies in the range of 0.5m to 100m depending of the receiver and the number of satellites visible. The computed coordinates are expressed using WGS 84 system.

3. Sensors miniaturization

The need for increasing miniaturization of electronic devices in order to use them in everyday tools, miniature robots and UAVs is foreseen to be stopped for a few years before

jumping further from the micro to nano-sized devices. Therefore a currently available at the market inertial measurement units need a review. There are multiple commercial inertial measurement units available at the market. For instance 3DM-GX 1 from MicroStrain, MTi-G from Xsens Technologies, Crista IMU from Cloud Cap Technology, μ NAV from Crossbow Technology, AHRS200AV2.5 from Rotomotion and ADIS 16400/405 from Analog Devices. In order to verify the capabilities of the mentioned solutions we have compared its characteristics with the current state of the art miniature MEMS IMU 5 developed by authors of the text. The comparison is visible in the tab. 1.

The current state of the art IMU 5 10-DOF allows for measuring angles in three dimensions, accelerations also in three dimensions, direction of the strongest magnet signal and the temperature of the surroundings. It utilizes MEMS technology in order to reduce both size and weight of the sensor. The sensor weighs only 1.13 [gram] without mounting and 3.13 [gram] with the standard mounting.

Measurement data from the IMU 5 sensor depending of the version can be sent through the USB or CAN bus or RS-232 which are typical industry standards of data transfer. The flexibility is required from modern sensors in order to integrate it with an existing systems. For the same reason the sensor has a flexible output data configuration. The output of the sensor can be acquired in three versions: as raw sensor data, as data after calibration and temperature compensation, or as the output of processing filter. Data from the sensors, may also be delivered in various forms to the user. The first form is the rotation matrix, which is generated based on data from the device. Data can also be supplied to the end user in the form of Euler angles and their values given in degrees or in radians. The third type of output data representation is by using quaternions.

Scheme of the operation of the micro measurement unit is presented in fig. 3 and the internal characteristics in tab. 2.

One of the fundamental inertial sensors is gyroscope measuring angular velocity Ω (in the schema GYRO(X), GYRO(Y), GYRO(Z)). Those sensors were oriented in such a way that their measurement axes create right handed Cartesian coordinate system. Analog MEMS type signals output is filtered by configurable low-pass filter (12.5, 25, 50, 110 Hz). After filtration the signal is converted into the digital form by analog-digital converter characterized by 16 bit resolution. The digital signal can be further filtered by configurable low and high-pass filters. The frequency of data from the gyroscopes can be set to 100, 200, 400 or 800 Hz. The resolution of the measurements can be configured with a modified precision in the range from 250 °/s to 2000 °/s.

Another important element in the schema is linear accelerations sensors block (in the schema ACC(X), ACC(Y), ACC(Z)). The sensors were oriented in such a way that the measurement axes also create right handed Cartesian coordinate system. Analog signals from the sensors MEMS output were redirected to the filter and further to the analog-digital converter. Maximum resolution of the measured accelerations can be configured to $\pm 2/\pm 4/\pm 8$ [g] ($g \approx 9.81\text{m/s}^2$). Accelerometers sensitivity was measured as 1 [mg].

Producer	MicroStrain	Xsens Technologies	Cloud Cap Technology
			
Model	3DM-GX1	MTi-G	Crista IMU
Internal sensors	accelerometers, gyroscopes, magnetometers, temperature sensor	accelerometers, magnetometers, gyroscopes, GPS	accelerometers, gyroscopes, temperature sensor
Gyroscopes range	$\pm 300^\circ/\text{sec}$	$\pm 300^\circ/\text{sec}$	$\pm 300^\circ/\text{sec}$
Accelerometers range	$\pm 5 \text{ g}$	$\pm 5 \text{ g}$	$\pm 10 \text{ g}$
Digital output	RS-232, RS-485	RS-232, USB	RS-232, CAN
Temperature range	-40°C to $+70^\circ\text{C}$	-20°C to $+60^\circ\text{C}$	-40°C to $+70^\circ\text{C}$
Size with mounting [mm]	64x90x25	58x58x33	52.07x38.8x25.04
Weight [gram]	75	68	38.6
Producer	Crossbow Technology	Analog Devices	Rotomotion
			
Model	μNAV	ADIS 16400/405	AHRS200AV2.5
Internal sensors	accelerometers, gyroscopes, magnetometers, temperature sensor, GPS	accelerometers, magnetometers, gyroscopes, temperature sensor	accelerometers, gyroscopes, magnetometers
Gyroscopes range	$\pm 150^\circ/\text{sec}$	$\pm 75\text{--}300^\circ/\text{sec}$	$\pm 90^\circ/\text{sec}$
Accelerometers range	$\pm 2 \text{ g}$	$\pm 18 \text{ g}$	$\pm 2 \text{ g}$

Producer	MicroStrain	Xsens Technologies	Cloud Cap Technology
Digital output	RS-232	SPI	RS-232, Ethernet
Temperature range	-5°C to +45°C	-40°C to +85°C	-5°C to +75°C
Size with mounting [mm]	57x45x11	31.9x23.5x22.9	>100x100x100
Weight [gram]	33	16	>100

Table 1. Comparison of currently available at the market miniature inertial measurement units.

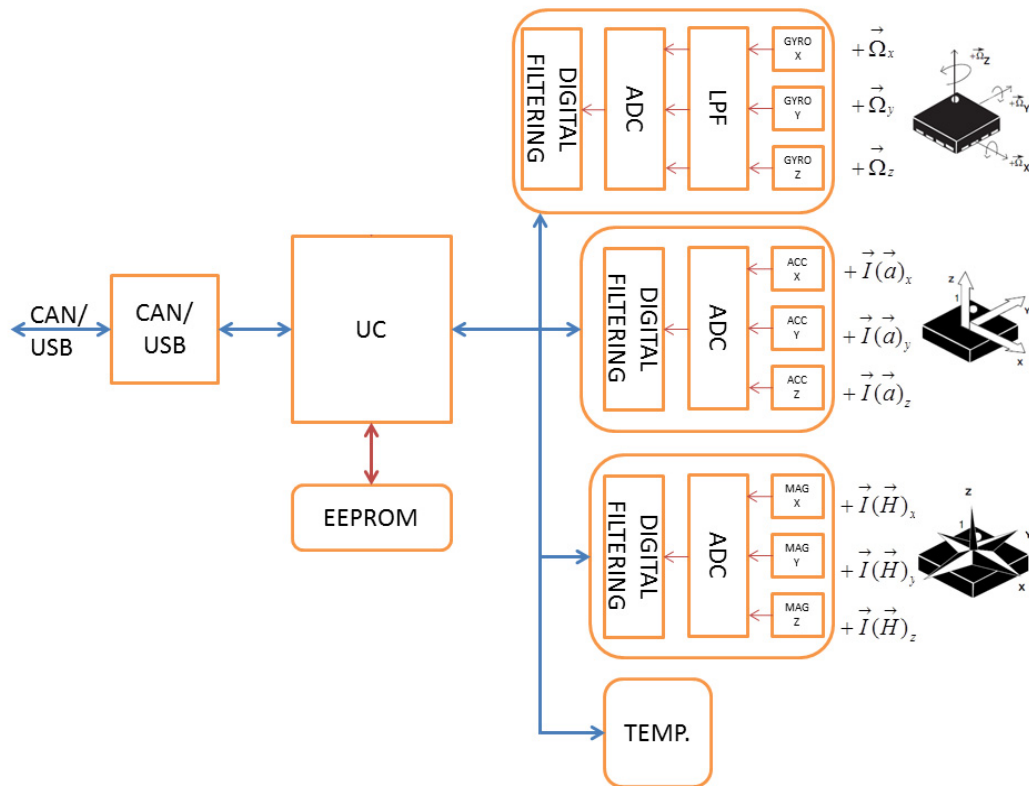


Figure 3. The IMU schema of operation.

Next functional block measures Earth magnetic field by using magnetometers (in the schema MAG(X), MAG(Y), MAG(Z)). Measurement axes of the sensors are oriented in right handed Cartesian coordinate system. The analog output from the sensors is connected with analog-digital converter and further with configurable filters block. Maximum values possible to measure are in the range from 1.3 to 81. [gauss] with resolution of 1/1055 [gauss].

The last functional block contains thermometer that measures temperature in the IMU's environment in order to allow for temperature compensation of the accelerometers, gyroscopes and magnetometers readings.

All of the functional blocks are connected with the central processing unit marked in the schema uProcessor. In order to store the required for algorithms parameters additional

memory was added (marked in the schema as eeprom). The CPU performs the filtering before the data is redirected to the CAN or USB or RS-232 output. In order to establish the parameters of the filtering algorithm the calibration phase is required.

Internal sensors	accelerometers, gyroscopes, magnetometers, temperature sensor	Gyroscopes range	from ± 250 to 2000°/sec
Accelerometers range	from ± 2 to ± 8 g	Digital output	CAN, USB or RS- 232

Table 2. Internal characteristics of the presented inertial measurement unit.

The presented IMU sensor volume is below 2cm³ with housing and weighs 3.13[gram]. Such size of the sensor can allow designers of robots to move from devices of considerable size to the designs of the micro scale. Maximum acceleration sensor is capable to withstand is 500 [g], while the input voltage is from 3.5 to 8V, and the current consumption is 35 mA. There are three different types of the housing that allows attachment of the sensor in various places. The smallest one Micro version (fig. 4) size with mounting is 18.6 x 14.7 x 7.3 [mm]. Version with the additional mounting holes Micro-Mounting version (fig. 5a) is 18.6 x 20.7 x 7.3 [mm]. The housings of Micro version and Micro-Mounting version output cable is appointed with the USB or RS-TTL connector depending of the version. There is also extended version with mounting holes and a LEMO plug embedded in the housing (fig. 5b). Its size is 32.0 x 18.0 x 16.5 [mm].

Physical measurements of all versions are presented in Tab.3.

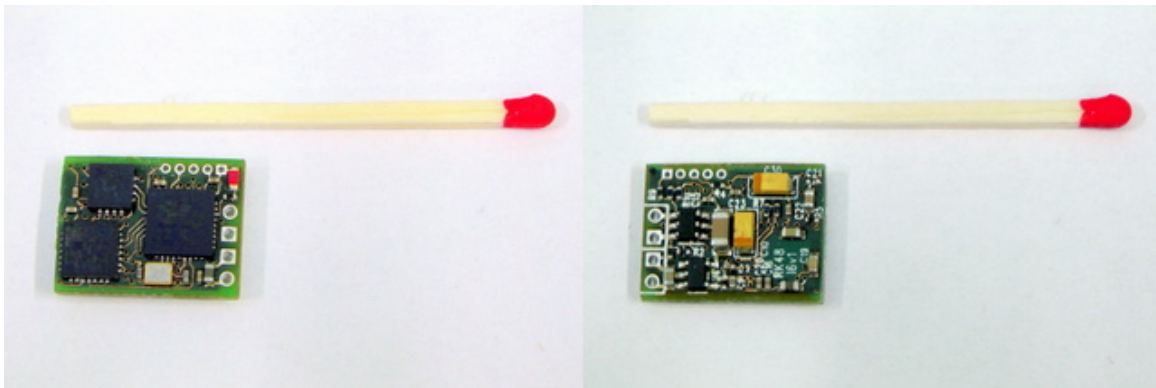


Figure 4. The front and back side of the inertial measurement unit.

Calibrated axes orientations are engraved and colored on the top side as presented in Fig. 5. Size of the single mounting is 6.15 mm for Micro-Mounting Version, and 6.50 mm for Extended LEMO version.

Before the application of the IMU in the physical objects a comparison between the smallest available at the market sensors was made in order to verify the possibility of navigation of autonomous mobile vehicles. Comparative studies were designed to check the parameters

set up the prototype, analyze the causes of measurement errors and to check how the sensors, which performed tests behave in extreme situations. For the tests two popular commercial miniature sensors were used: MTiG-28G from XSens Technologies and Crista IMU from Microstrain (fig. 6b).

IMU type	Dim. X	Dim. Y	Dim. Z	Units	Volume
Micro version	18.6	14.7	7.3	mm	1,996 cm ³
Micro-Mounting version	18.6	20.7	7.3	mm	2,811 cm ³
Extended version	32.0	16.5	18.0	mm	9,504 cm ³
Common parameters	Min.	Type	Max.	Units	
Weight (w/o housing)	-	1.13	-	gram	
Weight (w/ housing)	-	3.13	-	gram	
Operation temperature	-40	-	80	°C	
Storage temperature	-60	-	100	°C	
Maximal acceleration	-	500	-	g	
Input voltage	3.5	5.0	6.0	V	
Current	30	35	40	mA	

Table 3. Physical characteristic of the sensor.

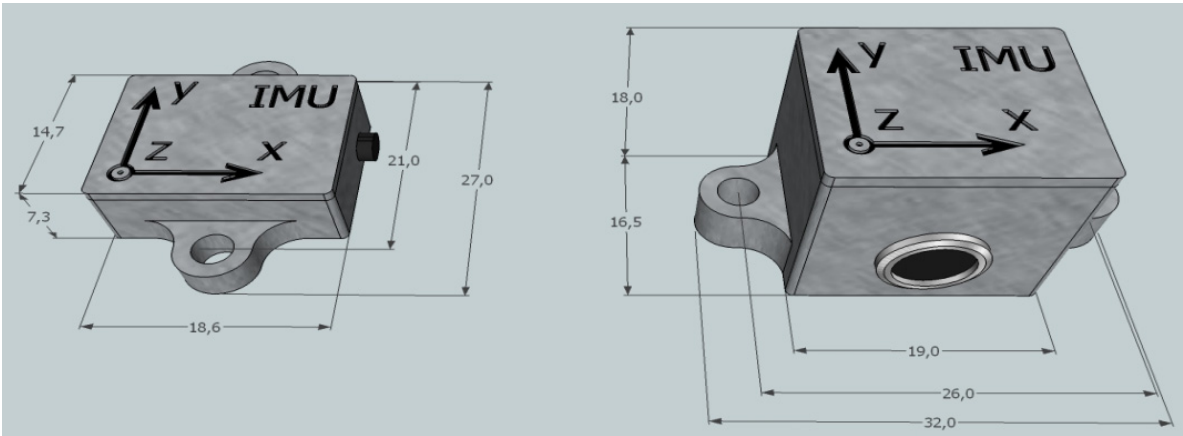


Figure 5. The micro IMU mounting schema. a) Micro-Mounting version, b) Extended LEMO version.

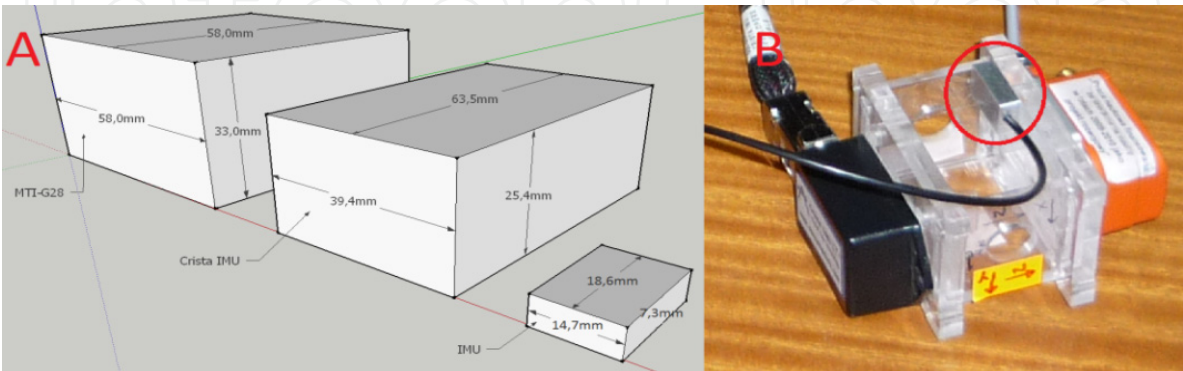


Figure 6. A) Comparison of the presented IMU size to the products available at the market, b) IMU comparison platform. The presented IMU is marked by the red ellipse. In the left side of the image Crista IMU can be seen. On the other side one can see MtiG Imu from XSense Technologies.

In order to perform comparative studies calibration platform was designed, produced and used (fig. 6b). All the tested IMU's were mounted to the platform and their raw data was calibrated to the common coordinate system for all the sensors using the presented calibration method. Several tests were performed: the raw data comparison, the filtered data comparison, time stability of the sensors and capability for temperature compensation. In the fig. 7a it is presented comparison of the readings from the accelerometers of the presented IMU sensor (CZK in the chart) and the MTiG sensor (MTI in the chart) and in the fig. 7b is presented the comparison of gyroscopes. Both comparisons were recorded during motion.

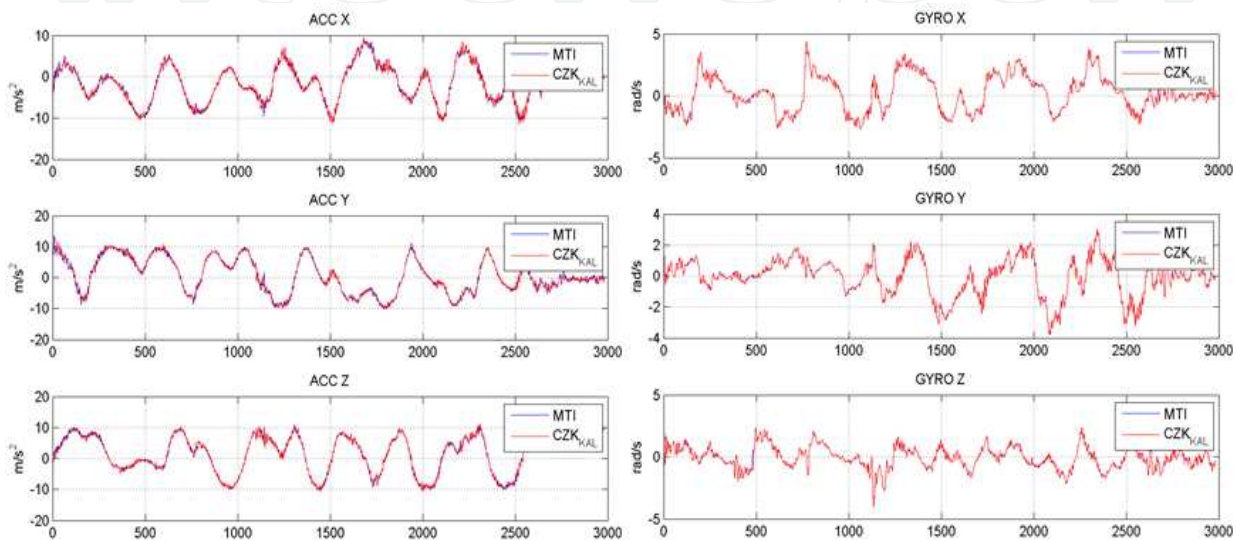


Figure 7. An example chart from comparative studies of the presented IMU sensor and the sensors available in the market. Presented IMU sensor is labeled as CZK and MTiG sensor from XSens Technologies is labeled MTI. Time units are [ms]. a) the readings from the accelerometers, b) the readings from the gyroscopes.

It can be noticed that the output data from the presented calibrated sensor and the reference sensor is almost the same. In order to measure the differences we have estimated the signal from raw data and separated it from the noise component. Only gyroscope Y measurement axe was chosen as an example for presentation. The chose was possible because achieved results are comparable regardless the axe and the sensor (magnetometers, accelerometers or gyroscopes). In the right part of the fig. 8 it is presented that standard deviation of the noise for MTi-G28 and our sensor is about 0.04 while the Crista IMU's result is about 0.12. The difference between standard deviation of MTi-G28 and our sensor is only 0.0035 which is usually undistinguishable by human eye.

Additional table collation of the signal to noise coefficient is presented in tab. 4.

An important problem for inertial measurement units is time stability of the output data. We have performed a series of stability tests with duration of 4h. The presented in the fig. 9 results were acquired after averaging from five samples of each IMU in the test. Two main observations can be made. First that MTi-G28 and our IMU results are comparable. The

achieved average values difference is only 0.00027 and the difference between standard deviation values is 0.00226 which is even lower than during the test with movement. The second observation is that our sensor and MTi-G28 results are more than 20 times closer to the real 0 value.

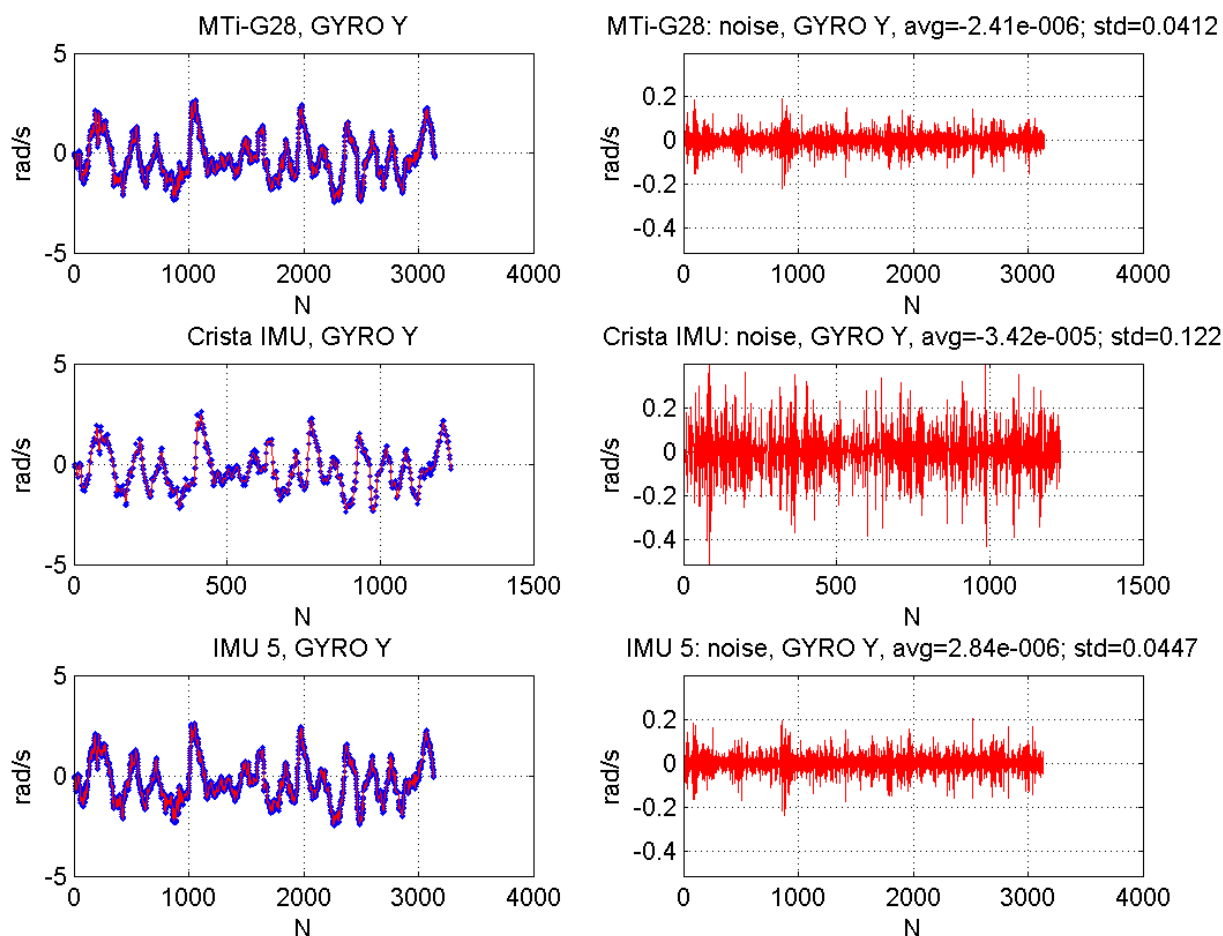


Figure 8. The comparison of the output data during movement from Y axe of gyroscopes for the tested sensors (MTiG-28, Crista IMU and our sensor). Time units are [ms].

	Crista IMU (S/N _{KAL})	MTiG (S/ N _{KAL})	IMU 5 (S/N _{KAL})
Accelerometers	20,3	38,1	43,2
Magnetometers	N/A	719,3	767,9
Gyroscopes	13,6	206,7	254,5

Table 4. The comparison of signal to noise coefficient for the tested IMUs. (The larger the value the better).

The global availability of the GPS, relatively high reliability of the readings and no need for additional infrastructure are the main reasons that most of the modern inertial navigation systems use GPS. The INS typically can be characterized by fast update rate and small but unbound error. GPS error is bounded however update time is slow and attitude estimation

is not reliable. Because of the closed architecture of the most of GPS modules the most popular method type of fusion methods is called uncoupled or loosely coupled aiding. INS with GPS is used in vehicle safety systems for estimation of a vehicle sideslip. The standard usage involves vehicle guidance and navigation. GPS signal requires a clear visibility of the satellites which is often not possible in the canyons, especially in urban canyon environments. The GPS/INS systems are often utilized for navigation of a quadcopter or missile guidance.

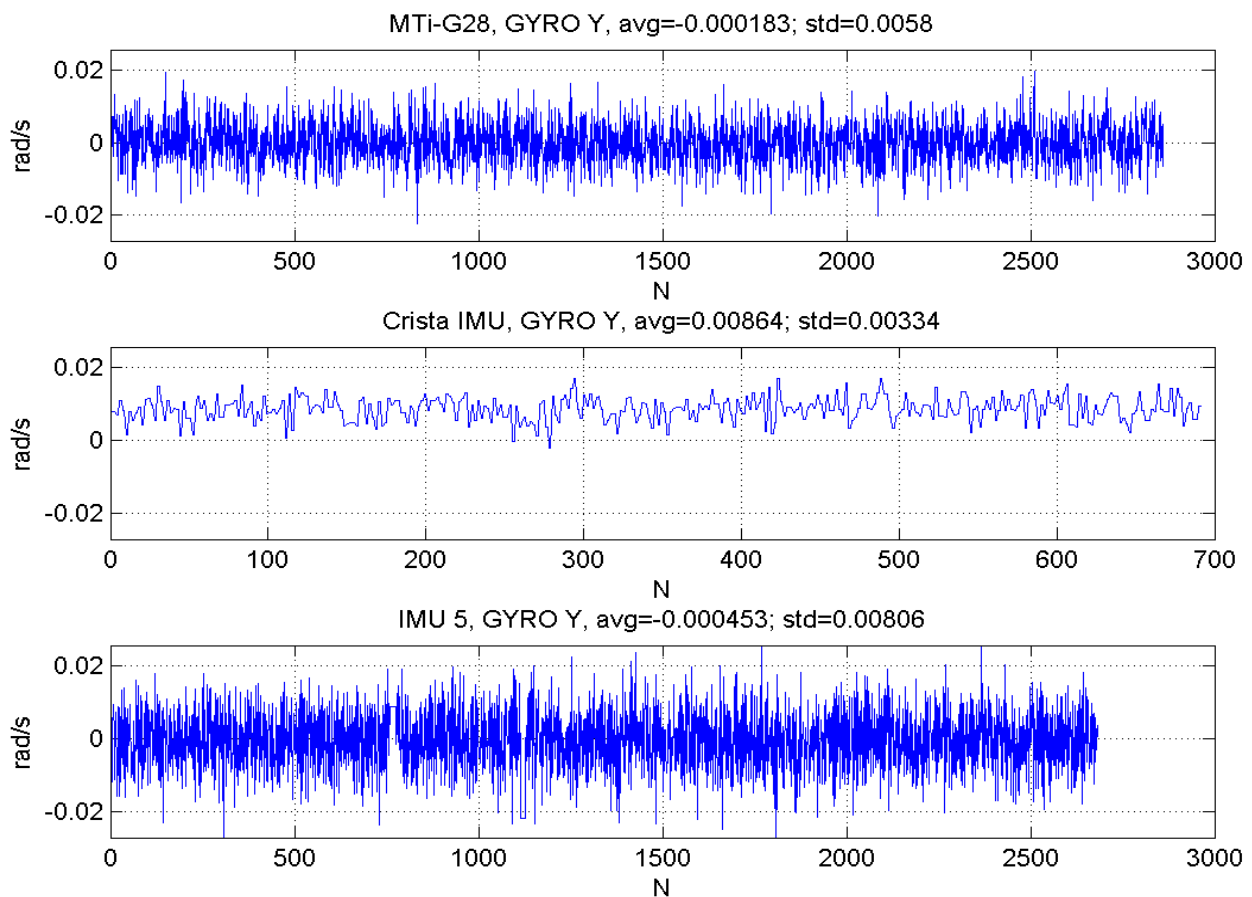


Figure 9. The comparison of the output data during stability test from Y axis of gyroscopes for the tested sensors (MTiG-28, Crista IMU and our sensor). Each value in the chart is an average value of 5 samples from the sensor.

We have developed an inertial navigation system as a complete navigation solution embedded in a single PCB. It contains 10-DOF inertial measurement unit presented above accompanied by Global Positioning System (GPS) module. In order to compensate for the low precision of the altitude estimation of the GPS additional barometer was embedded. The described INS allows for measuring angles in three dimensions, accelerations also in three dimensions, direction of the strongest magnet signal and the temperature of the surroundings. It utilizes MEMS technology in order to reduce both size and weight of the sensor. The INS printed circuit board with MCX connector weighs 3.67 gram without mounting and 8.86 gram with the standard mounting.

Measurement data from the sensor depending on the version can be sent through the USB or CAN bus which are typical industry standards of data transfer. The flexibility is required from modern sensors in order to integrate it with an existing systems. For the same reason the sensor has a flexible output data configuration. The output of the sensor can be acquired in three versions: as raw sensor data, as data after calibration and temperature compensation, or as the output of processing filter. Data from the sensors, may also be delivered in various forms to the user. The first form is the rotation matrix, which is generated based on data from the device. Data can also be supplied to the end user in the form of Euler angles and their values given in degrees or in radians. The third type of output data representation is by using quaternions. The output position coordinates from the GPS are sent in the Earth Centered Earth Fixed (ECEF) coordinate system. The unit of the estimated speed by the GPS is m/s. The used embedded atmospheric pressure altimeter is characterized by internal temperature compensation. It allows for measuring the atmospheric pressure in the range from 20 to 110 kPa with resolution of 1.5 Pa. It can be used to estimate the altitude of the sensor with a resolution equals to 30cm. Geographical localization of the sensor is computed using the GPS module. The GPS is connected to the microprocessor by serial communication bus. In order to improve the quality of the coordinates estimation it is possible to pass to the GPS differential corrections (DGPS). The output from the GPS is in Earth Centered Earth Fixed (ECEF) coordinate system and the frequency is 10 Hz.

The presented INS sensor volume is below 4cm³ with housing and weighs 8.86 [gram]. Such size of the sensor can allow designers of robots to move from devices of considerable size to the designs of the micro scale. Maximum acceleration sensor is capable to withstand is 500 [g], while the input voltage is from 3.5 to 8V, and the current consumption is 50 mA. There are two different types of the housing that allows attachment of the sensor in various places. The smallest one Micro version (fig. 10) size with mounting is 32.7 x 14.9 x 8.0 [mm]. Version with the MCX connector (fig. 3b) is 32.7 x 14.9 x 12.1 [mm]. The volume of the extended version is below 6cm³. The sensor can operate in a wide range of temperatures starting from -40°C to 80°C.

Physical measurements of all versions are presented in Tab.5.

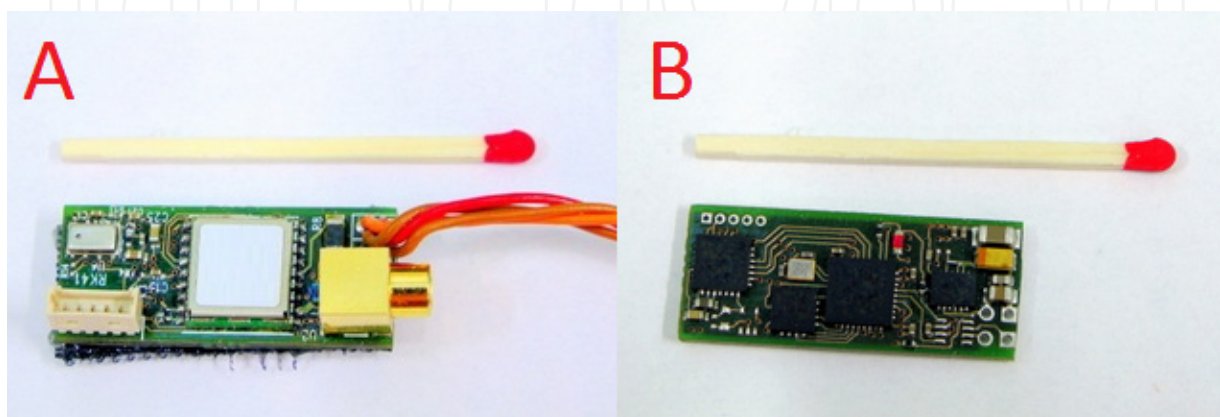


Figure 10. The front (a) and back (b) side of the inertial navigation system PCB with MCX connector.

INS type	Dim. X	Dim. Y	Dim. Z	Units	Volume
Micro version	32.7	14.9	8.0	mm	3.897 cm ³
Extended version	32.7	14.9	12.1	mm	5.895 cm ³
Common parameters	Min.	Type	Max.	Units	
Weight (w/o housing)	-	3.67	-	gram	
Weight (w/ housing)	-	8.86	-	gram	
Operation temperature	-40	-	80	°C	
Storage temperature	-60	-	100	°C	
Maximal acceleration	-	500	-	g	
Input voltage	3.5	5.0	6.0	V	
Current	40	50	60	mA	

Table 5. Physical characteristic of the sensor.

Calibrated axes orientations are engraved and colored on the top side as presented in Fig. 11.

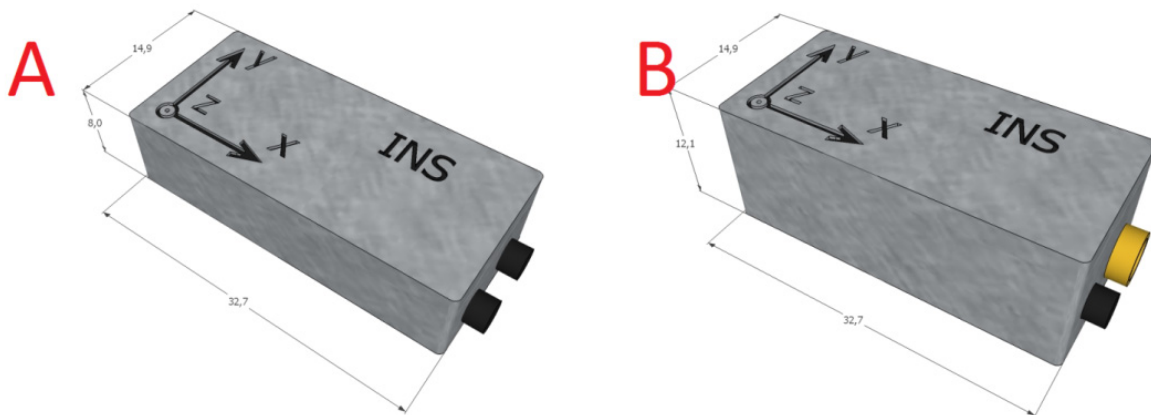


Figure 11. The INS mounting schema. a) Micro-Mounting version, b) Extended version.

The introduced INS was compared against the smallest IMU with a volume below 2 [cm³]. Both the measurement and size axes are marked in the fig 12ab. The X dimension of the micro IMU 5 is 18.6 [mm] which is about 57% of the INS size. The Y dimension is 14.7 [mm] which is about 99% of the INS size and the Z size of the IMU is more less equal to 91% of the Micro version of the INS and 60% of the Extended version. However the Extended LEMO version of the IMU is 18 [mm] which is 225% of the micro version of the INS. Comparison based on the volume only allows the statement that the micro version of the INS is less than two times larger (195% of the micro version of the IMU).



Figure 12. The comparison of the proposed INS (b) with the World's smallest IMU (a). The measurement axes are drawn in the image. c) The comparison of the mounting's size of the presented INS and IMU, d) The comparison of the external characteristics of the proposed INS and the IMU.

4. GPS and INS data fusion

Inertial measurement units are commonly used as a separate tools. However IMUs are also often used as a supplying unit for positioning systems e.g. Global Positioning System (GPS). GPS signal accuracy is not sufficient for object's precise navigation. Estimated position is biased with a large error especially on altitude signal's component. The error can be as high as hundred meters depending on the number of the satellites in the field of view of the GPS receiver. GPS is also not capable of working inside of buildings or in tunnels. There is no acceleration and orientation data. All the lacking information required for precise navigation can be obtained from IMUs. The integration of GPS and IMU into one system called inertial navigation system (INS) is usually implemented in one of two ways: loosely coupled and tightly coupled. Loosely coupled type consists of independent components with additional piece of software which allows sharing program resources. In such systems, application logic is implemented in loosely integrated group of communicating devices. Each device has its own local memory. The system is usually based on Kalman filter processing data from GPS and IMU altogether. Readings from GPS are treated as a reference fix information. As a counter measure for IMU error accumulation simplified schema is presented in fig. 13.

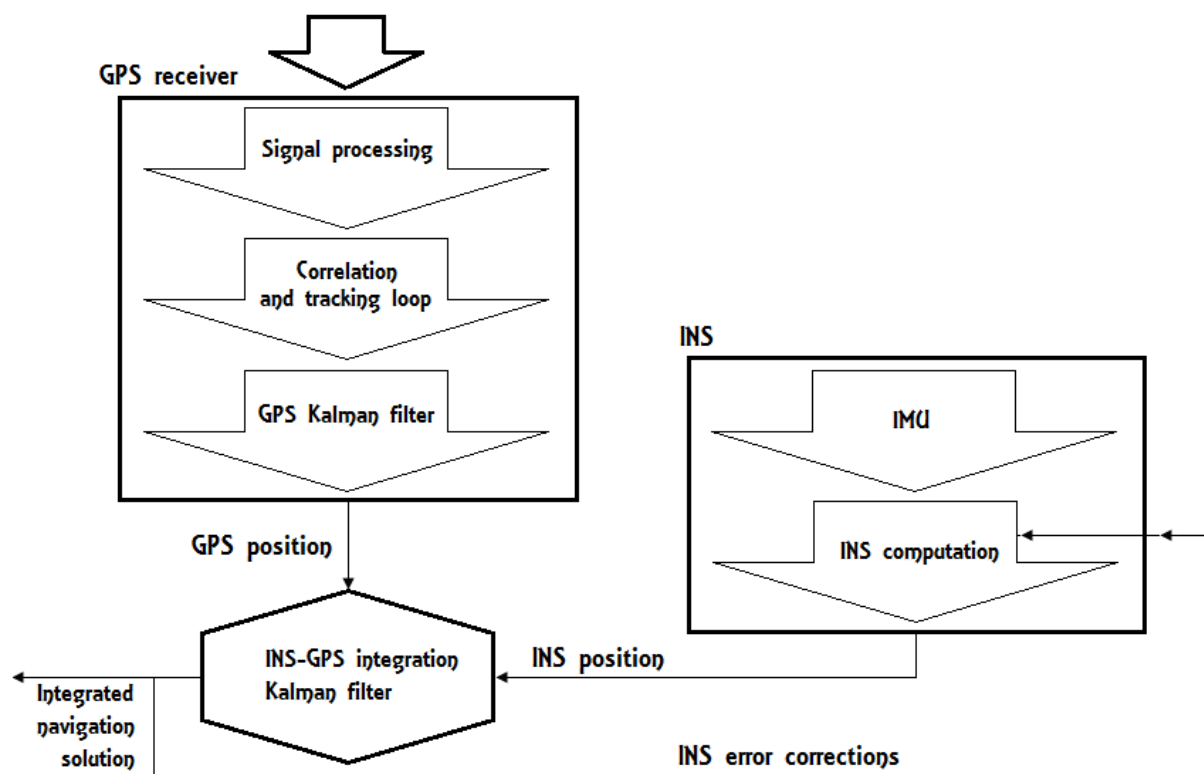


Figure 13. Loosely coupled integration type schema.

One of the most significant advantages of a loosely coupled system is a possibility to share resources among system nodes. Computation speed and reliability can be increased because of distributed processing. In case of error of one components the rest is still operating,

therefore the overall reliability is increased. Communication network among the nodes allows to distribute information.

Tightly coupled systems are integrating GPS and IMU in one system with a central shared memory. Each of the devices can exist in common memory hierarchy. Inertial measurement units are used for measuring objects' orientation and acceleration and estimating velocity and position using navigation equations. Computed parameters aids readings, called pseudo-ranges, from the GPS receiver. After correlation, both signals are used by an integration Kalman filter. Simplified schema of the tightly coupled solution is presented in fig. 14. Due to INS corrections, GPS receiver in the system can work also when visible satellites are in range from one to four as good as it is working usually with five and more reference points visible. However accuracy of the systems increases with the number of visible satellites.

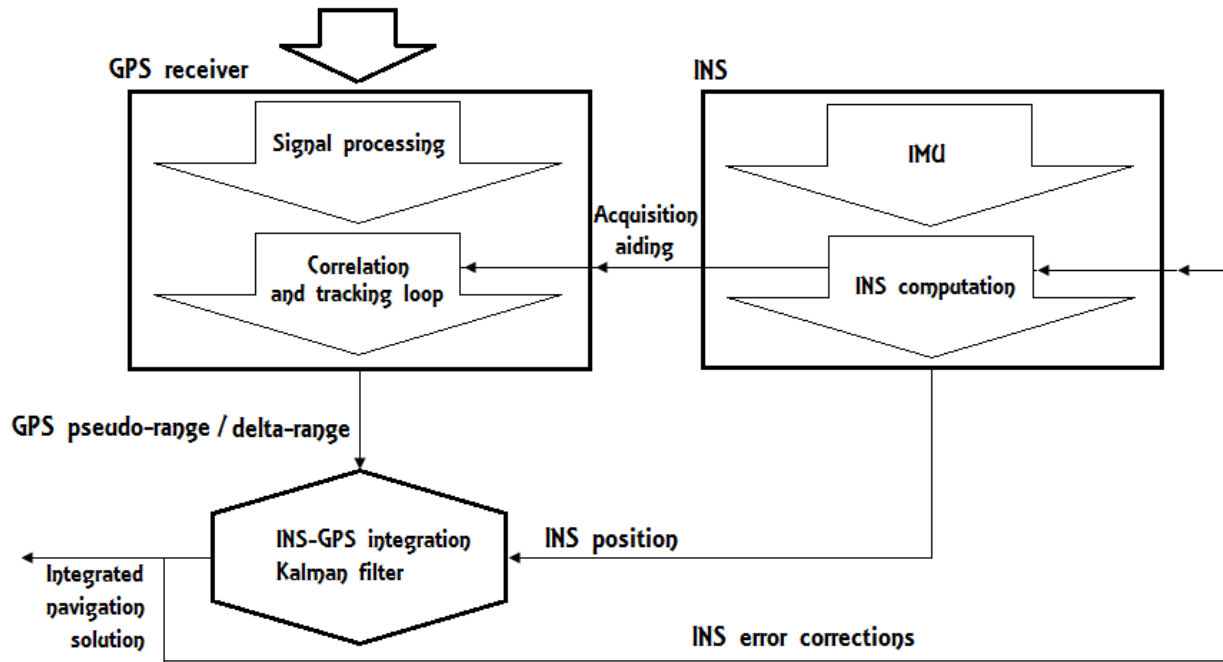


Figure 14. Tightly coupled integration type schema.

Many significant advantages of inertial measurement units can be found. The main advantages are high amount of possible applications, micro size and weight, high quality of data measurement. Due to those features IMUs are gaining more scientific attention each year and are implemented in various applications all over the world.

The dynamic model of the INS-GPS loosely coupled system can be formed from the differential equations of the navigation error. The time-varying stochastic system model is

$$\begin{aligned}
 \dot{x}_{INS}(t) &= F_{INS}(t) + G_{LC}(t)b(t) + G_{LC}(t)w_{LC}(t), w_{LC} \sim N(0, Q_{LC}) \\
 x_{INS} &= [\delta L \quad \delta l \quad \delta h \quad \delta V_N \quad \delta V_E \quad \delta V_D \quad \theta_N \quad \theta_E \quad \theta_D]^T, \\
 w_{LC} &= [w_{aX} \quad w_{aY} \quad w_{aZ} \quad w_{gX} \quad w_{gY} \quad w_{gZ}]^T
 \end{aligned} \quad (4)$$

where the error state variable $x_{INS}(t)$ represents the position, velocity, and attitude errors of a vehicle, the bias term $b(t)$ represents the inertial sensor bias errors, which consist of the accelerometer bias error and the gyro bias error, w_{LC} is the white noise of the inertial sensor with zero mean and covariance Q_{LC} . The system matrix $F_{INS}(t)$ and $G_{LC}(t)$ are

$$\begin{aligned} F_{INS} &= \begin{bmatrix} F_{11} & F_{12} & F_{13} \\ F_{21} & F_{22} & F_{23} \\ F_{31} & F_{32} & F_{33} \end{bmatrix} \\ G_{LC}(t) &= \begin{bmatrix} 0_{3 \times 3} & 0_{3 \times 3} \\ C_b^n & 0_{3 \times 3} \\ 0_{3 \times 3} & -C_b^n \end{bmatrix}, \end{aligned} \quad (5)$$

where the information of $F_{INS}(t)$ and $G_{LC}(t)$ is referred in. The accelerometer error consists of white Gaussian noise and the accelerometer bias error, which is assumed as a random constant. The gyroscope error consists of white Gaussian noise and the gyroscope bias error, which is also assumed as a random constant. The measurement model of the INS-GPS loosely coupled system uses the position and velocity information of the INS and the GPS as

$$z(t) = H_{LC}x_{INS}(t) + v_{LC}(t) = \begin{bmatrix} P_{INS} \\ V_{INS} \end{bmatrix} - \begin{bmatrix} P_{GPS} \\ V_{GPS} \end{bmatrix}, \quad v_{LC} \sim N(0, R_{LC}), \quad (6)$$

where $H_{LC} = [I_{6 \times 6} \quad 0_{6 \times 3}]$ and v_{LC} is the white Gaussian noise with zero mean and covariance R_{LC} .

5. Experiments

In order to present the performance of the INS-GPS loosely coupled system, experiments were done on the stadium near the Silesian University of Technology. The differential GPS (DGPS) trajectory with 2 m accuracy was used as a reference trajectory for quantitative comparison. All measurements were provided by the previously introduced micro INS. In order to make the test comparable with existing solutions the output data frequency from the GPS was set to 1 Hz as most of commercial civilian GPS receivers instead of the possible 10 Hz frequency. The path the vehicle passed was recorded and visible in fig. 15f.

Most of practical applications in order to perform INS-GPS data fusion use the well-known Kalman filter. However the Kalman filtering technique requires complete specifications of both dynamical and statistical model parameters of the system. This assumption in most of practical cases is not fulfilled. The measured values often deviate from their nominate values or have an unknown time varying bias. Such conditions seriously affect the Kalman filter estimates. In order to reduce the impact of the deviations a two stage Kalman Filter (TKF) was suggested. In order to extend TKF to nonlinear systems a new two-stage extended Kalman filter was introduced TEKF. However TEKF was only an approximation of EKF. In order to solve this limitation, Caglayan proposed a general TEKF, which

considers a general case in which the bias enters nonlinearly into the nonlinear system dynamics and measurements. Then, the bias is treated as not a random bias but a constant bias. An unknown random bias of a nonlinear system may cause a big problem in the TEKF because in a number of practical situations, the information of an unknown random bias is incomplete and the TEKF may diverge if the initial estimates are not sufficiently good. So the TEKF for a nonlinear system with a random bias has to assume that the dynamic equation and the noise covariance of an unknown random bias are known. To solve these problems, an adaptive filter can be used. The current state of the art algorithm is adaptive two-stage extended Kalman filter (ATEKF). The performance of the TEKF is the same as that of the EKF, as both filters are equivalent. However TEKF performance is significantly decreased when the bias is unknown or the sensor is temporary faulted which often happens in real life. Therefore we present the results acquired during the experiments when the bias was both known and unknown using both TEKF and ATEKF algorithms.

The navigation results using the ATEKF when there is no fault are presented in fig. 15. The partial figures show the position, velocity, attitude, an accelerometer bias, a gyroscopes bias, and a position error of the test vehicle used during the experiments. The position error is defined as the difference between a position of the DGPS and the computed value. The accelerometer bias and the gyroscope bias are both well estimated by the ATEKF. In order to perform the comparison of performance between the algorithms, the horizontal-axis average position error is defined traditionally as

$$e_T = \sqrt{\left(\frac{1}{T} \sum_{t_k=1}^T |e_N(t_k)|\right)^2 + \left(\frac{1}{T} \sum_{t_k=1}^T |e_E(t_k)|\right)^2}, \quad (7)$$

where e_N and e_E mean the position errors of the north and east axis, respectively. T is the total navigation time of the vehicle. The TEKF shows the horizontal-axis average position error of 4.70 m and the ATEKF shows 4.90 m for the INS-GPS loosely coupled system without an unknown fault bias. It was confirmed that the TEKF and the ATEKF show almost an equivalent performance for the integrated navigation system when the bias was known.

In order to test the performance of the ATEKF for GPS-INS data fusion in a loosely coupled system when the bias is unknown two situations were taken into consideration: fault of accelerometer and fault of gyroscope. A fault biases (10, 30, 50, 100 [mg]) were inserted into measured data from the X-axis of the accelerometer and (50, 100, 200, 300 [deg/h]) gyroscope.

Fig. 16 shows the navigation results of the INS-GPS loosely coupled system using the ATEKF when the accelerometer sensor had a fault. These figures show the position error in the TEKF and the ATEKF for the integrated navigation system with an accelerometer fault bias. As expected, the position error of the ATEKF was smaller than that of the TEKF. Fig. 17 shows the bias estimation results of the TEKF and the ATEKF for several accelerometer fault biases.

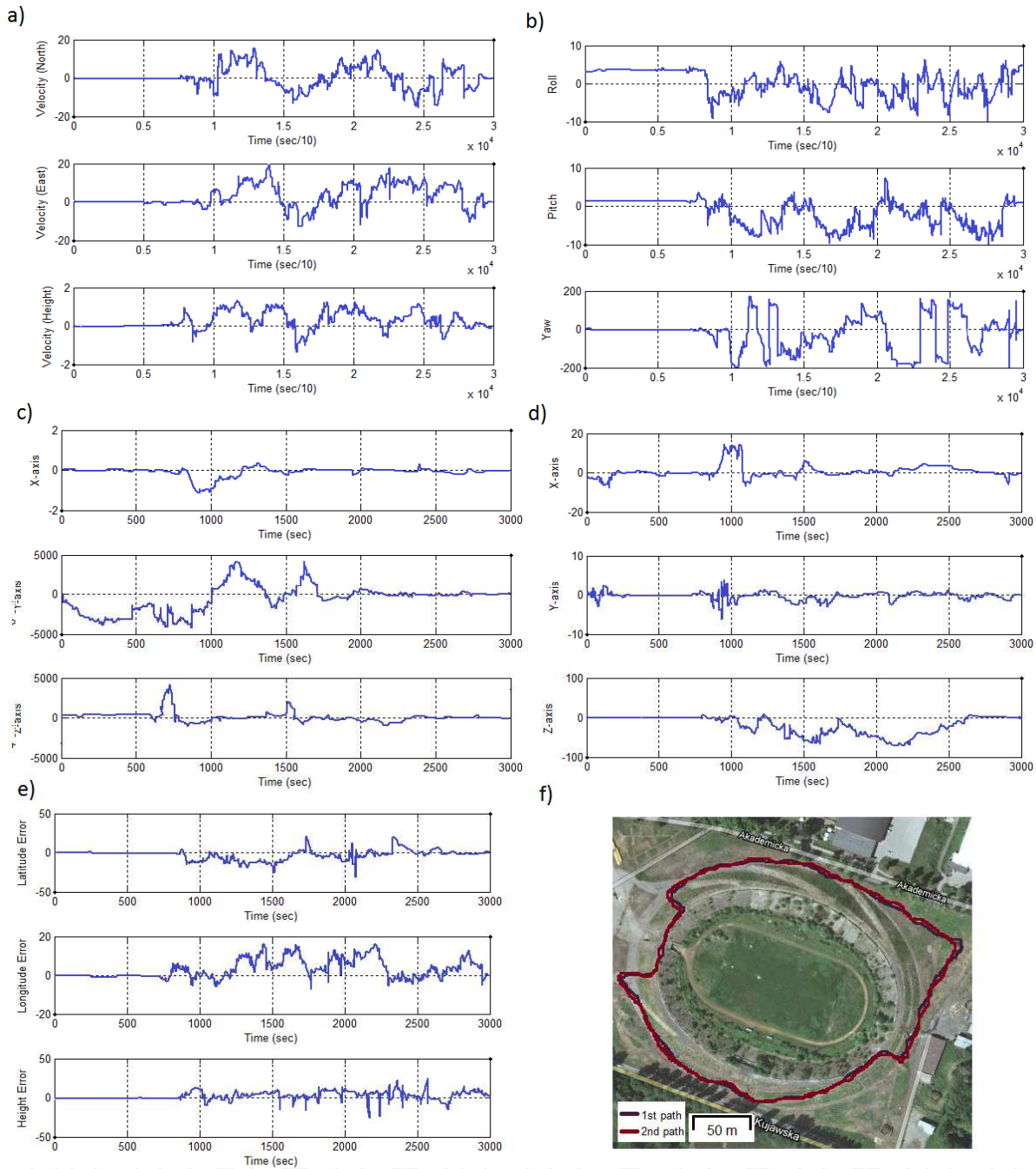


Figure 15. Results acquired using the ATEKF algorithm with known bias. a) Velocity, b) Attitude [deg], c) Accelerometer bias [μg], d) Gyroscope bias [deg/h], e) Position error [m], f) Path around the stadium.

It was evaluated that the tracking performance of the ATEKF was better than that of the TEKF. The ATEKF algorithm was capable of reliable tracking even with an unknown fault bias. The estimate of a fault bias was used for the compensation of the sensor fault, so the navigation error in the ATEKF was smaller than that of the TEKF. Fig. 18 shows the position error in the TEKF and the ATEKF for the integrated navigation system with a gyroscope fault bias. The total tendency was similar to the results in the accelerometer. Fig. 19 shows the bias estimation results of the TEKF and the ATEKF for several gyroscope fault biases. It can be observed in the figures 17 and 19 that the accelerometer bias converges faster than gyro biases.

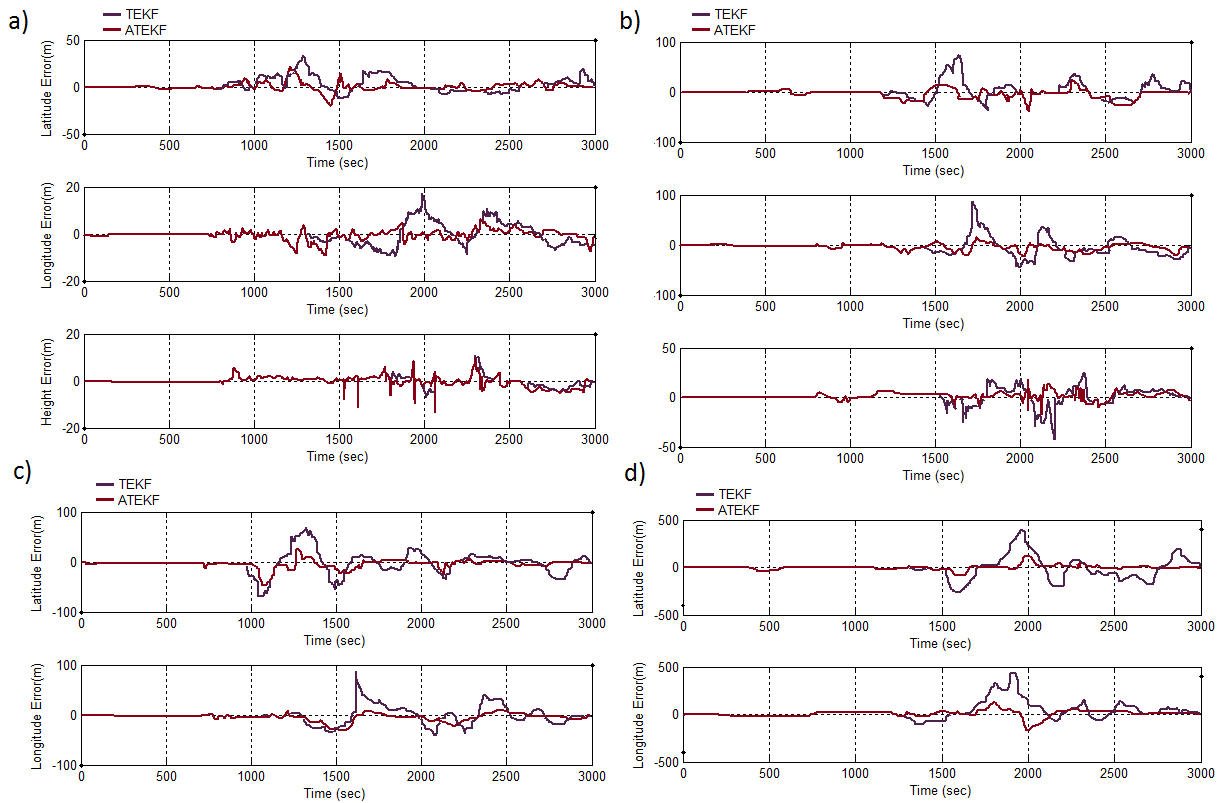


Figure 16. Comparison of the TEKF and ATEKF algorithms in case of accelerometer fault bias. a) X-axis bias 10mg, b) X-axis bias 30 mg, c) X-axis bias 50mg, d) X-axis bias 100mg.

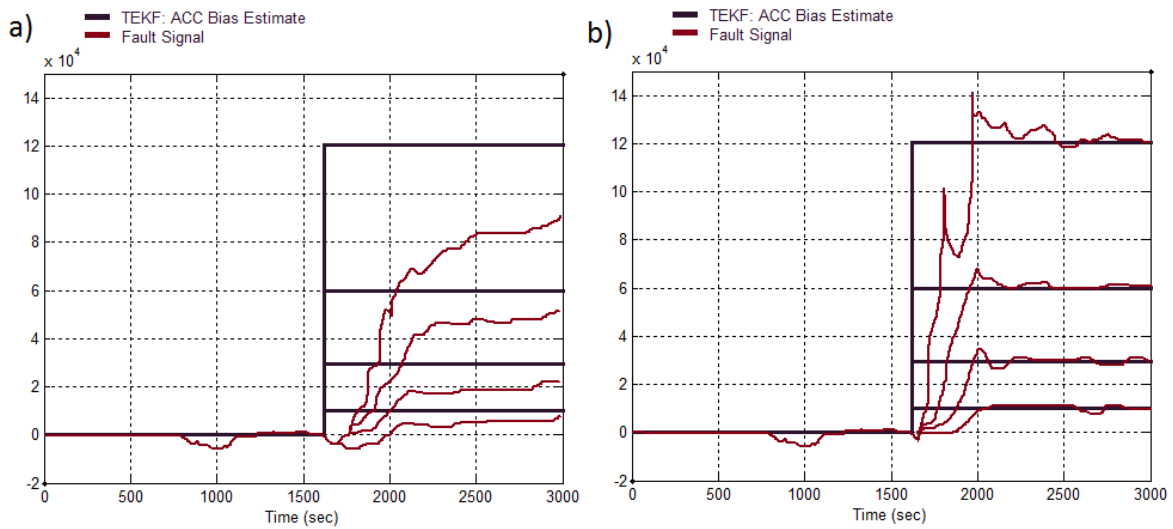


Figure 17. Comparison of the TEKF and ATEKF algorithms in case of several accelerometer fault biases. a) TEKF, b) ATEKF.

In the fig. 20 the response of the filter for a jumping fault bias are presented.

It was presented that the ATEKF filter successfully fuse together signals from accelerometers, gyroscopes and GPS in order to provide reliable and stable measurements required for many applications. Therefore it is justified to safely implement the algorithm in the sensors as it was done for the presented micro INS sensor.

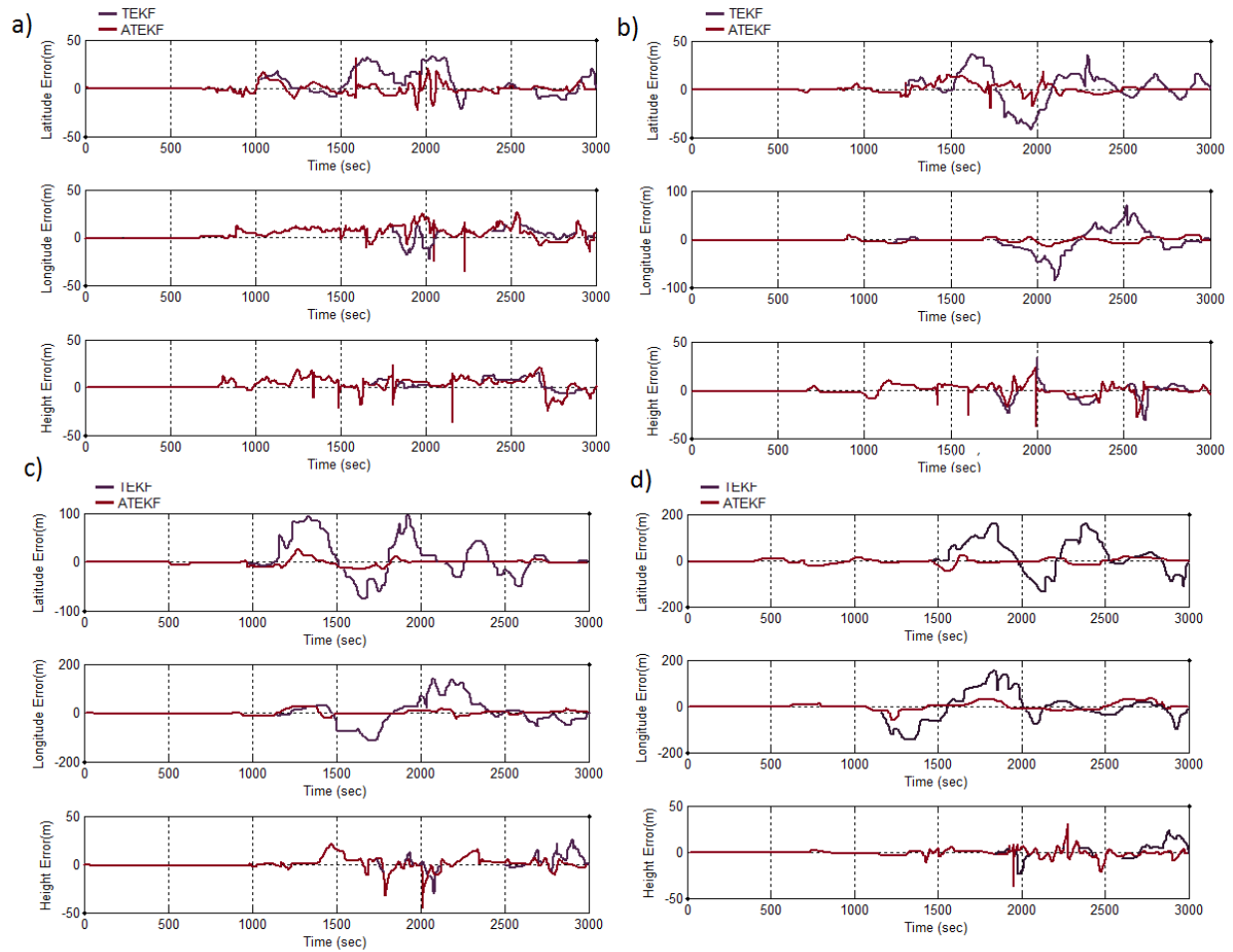


Figure 18. Comparison of the TEKF and ATEKF algorithms in case of gyroscope fault bias. a) X-axis bias 50deg/h, b) X-axis bias 100deg/h, c) X-axis bias 200deg/h, d) X-axis bias 300deg/h.

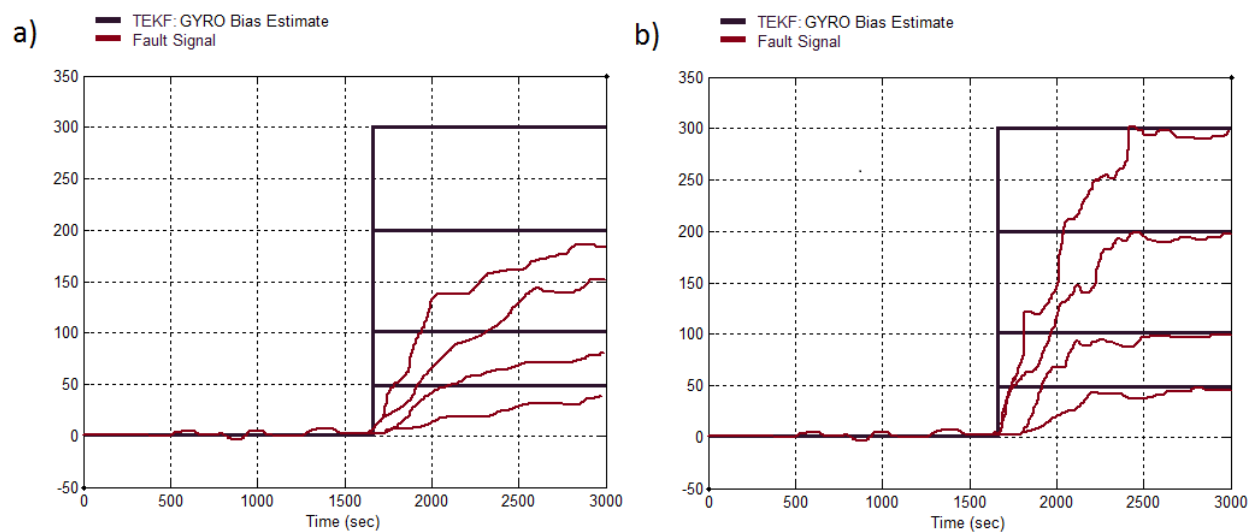


Figure 19. Comparison of the TEKF and ATEKF algorithms in case of several gyroscope fault biases. a) TEKF, b) ATEKF.

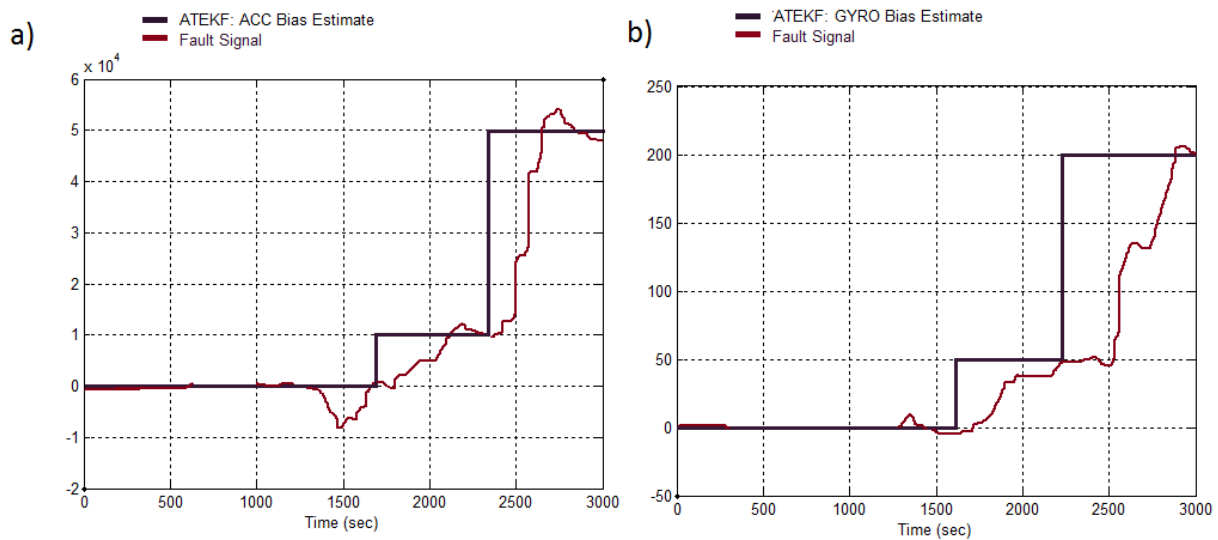


Figure 20. Results of the ATEKF algorithm acquired during fault bias jumping change. a) Accelerometer fault bias. b) Gyroscope fault bias.

6. Practical implementations

The most important in research is its practical application. After evaluation the quality of the inertial measurement units loosely coupled with the GPS receiver the next step was to implement it in real life application. IMUs are widely used in navigation various vehicles and objects. Application of the presented sensors for instance in autonomous navigation of unmanned flying or ground objects can be achieved by extending the approach presented in the experiments section. Main stream of current research in the field of inertial measurement units is to decrease the volume of the sensor in order to make it possible to use in different applications than navigation. Here we present few types of applications possible with the presented miniature sensors.

In order to verify the possibility of real-life application a challenging field was chosen. It was decided that the micro size of the IMU sensor will be used in sports. For instance in running. The sensor can be applied to each of the running shoes of the runner (fig. 21a-b). Alternatively the IMU can be placed on the wrist. It is worth mentioning that the runners were volunteers helping during the research. We have asked runners to test the application during the 4x100m relay race around the stadium. Each of four runners were equipped in the two IMUs. One on each of running shoes. The computed geographical trajectories are overlaid on the satellite view of the stadium. Using the output data from the system it was possible to record the exact path of each runner (fig. 21c). Therefore easily it was possible to calculate the time and velocity vector of each runner. The measured times are 11.89, 11.96, 12.10 and 12.01 and the average speed for all runners was 8,340 [m/s]. It can be seen that there is a movement of the runner while waiting for their turn (start without starting blocks) and after it. The start and stop of the recording was invoked remotely by radio communication and globally for all runners.

Encouraged by the success with the runner we have implemented a system for measuring statistics during football matches. It is important to be able to monitor the activity of each

player during and after the match. The collected offline data can easily be used in order to profile the quality and activity of the players during the match and therefore polish the chosen tactic for the match. The statistics are also often used during players recruitment. However the most important in our opinion are two applications of the collected data. First analyzing the reasons behind the injuries during the match and second online monitoring of the match in order to polish the team tactic in the real time by the coaches. Thanks to Piast Gliwice sport club courtesy we were able to record a football match played by professional players. Two players were playing at central midfield, one player at external midfield and forward field. A similar approach to those previously tested with runners was used. Each recorded player was equipped in two micro INS mounted on the shoes and wireless communication board. The new part was a software which allows wireless online monitoring of the variables of each INS, therefore the current activity of selected players. The collected data was used in order to compute the total walking time, total running time, average time of non-activity, average, minimum and maximum speed of running. Regardless the statistics the whole motion path data was recorded for more detailed tactics offline processing. Current implementation was limited to four players however the system can be easily extended to all players. Fig. 21 presents acquired data during the match. An interesting extension of the presented system would be its integration with vision system in order to collect multimodal data.

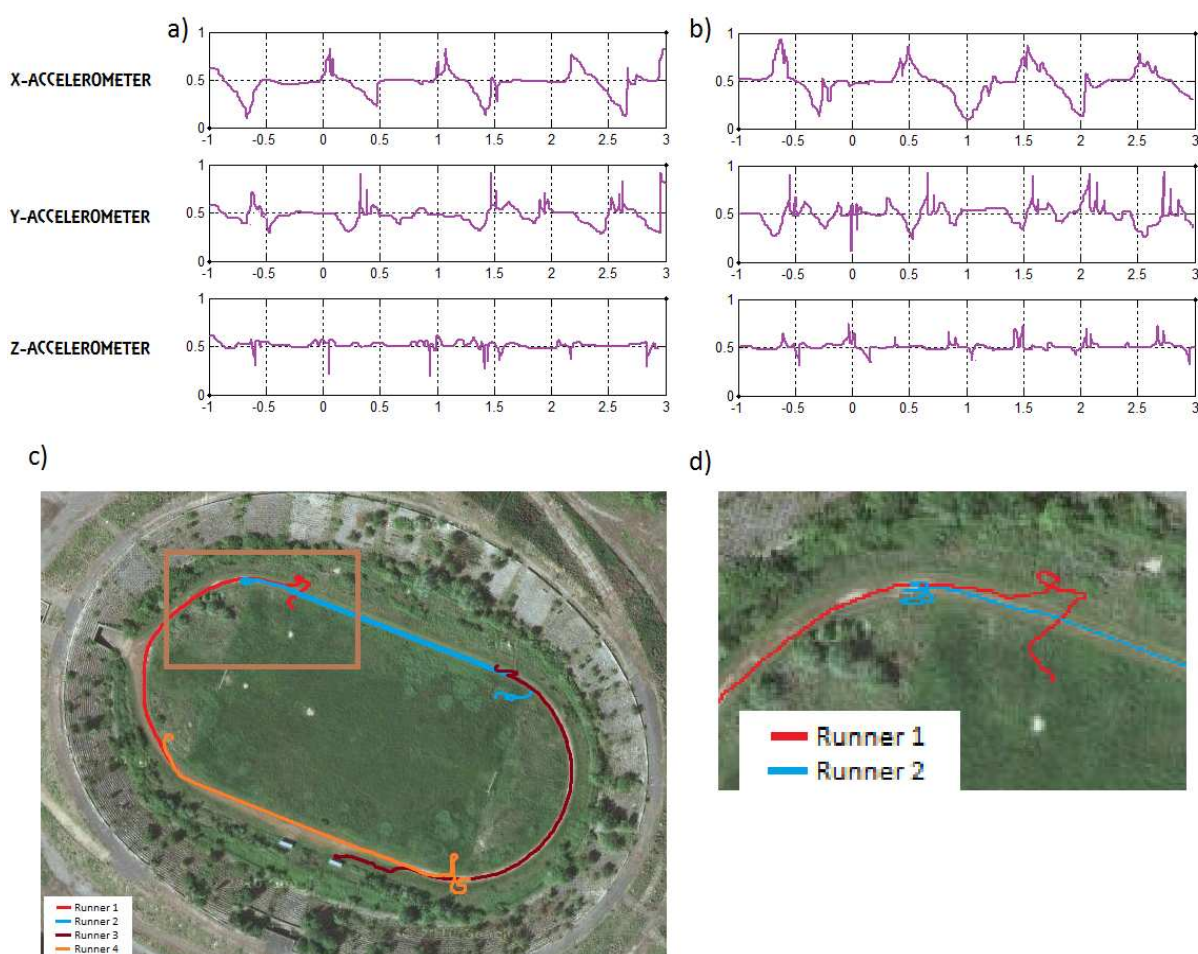


Figure 21. An example data collected during recording 4x100m relay race. a-b) accelerometer data during gait, c) the trajectory, d) zoom in the marked rectangle.

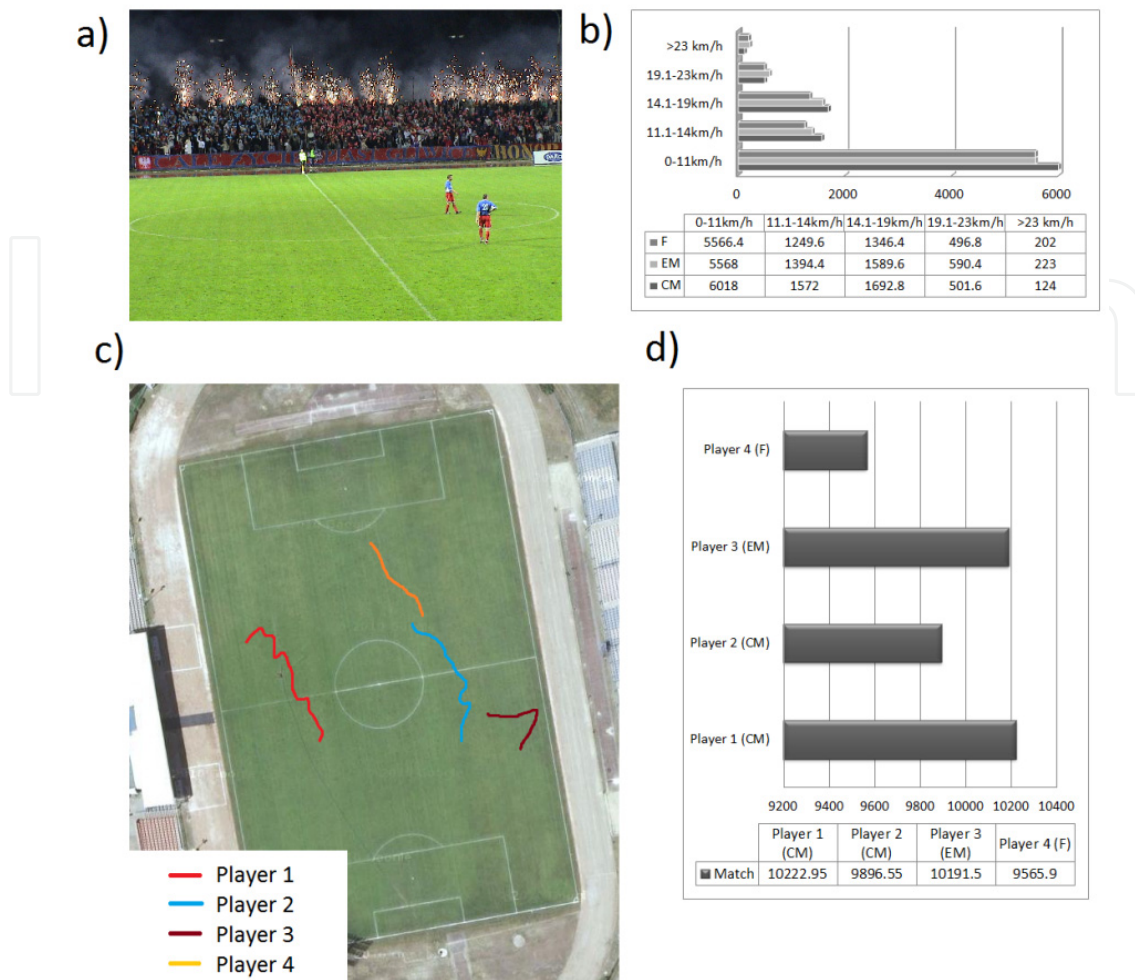


Figure 22. Motion paths acquired using the presented loosely coupled INS-GPS during the football match. a) Photograph from the match, b) distance covered by different types of players in different levels of activity, c) sample motion path overlaid on the satellite view of the stadium, d) total distance covered by different types of players.

7. Conclusions

The chapter presents the complete path of development of an example inertial measurement unit. The process of development includes: choosing algorithms of filtration and fusion, implementation and finally tests and practical applications. As a first step an analysis of existing solutions of algorithms for determining the orientation of the object in three dimensional space was performed. Acquired results allowed to select the technology capable of building a micro inertial measurement unit. Main criteria of selection was miniature size, therefore MEMS technology was chosen. Research team from Silesian University of Technology designed and produced two types of sensors. Micro inertial measurement unit IMU 5 for measuring object's orientation in the space and a second sensor INS extended with altimeter and the GPS receiver. Both presented devices can be distinguished by their many times smaller volume than the currently available at the market. However with smaller size comes no change in the quality of the solution. The next step of research was to design data fusion algorithm from data acquired from the inertial

measurement unit and the GPS. The algorithm was implemented in hardware of the sensors and extensively tested in various conditions and applications. The considerations presented in the chapter allow to confirm the possibility of using miniature MEMS sensors in real applications without need to worry about loss of measurement's precision. It was proved that using the presented algorithm it is possible to acquire high quality output data signal. Such output data could be applied to the various real life applications, for instance sport.

Author details

Aleksander Nawrat, Karol Jędrasiak, Krzysztof Daniec and Roman Koteras
Silesian University of Technology, Department of Automatic Control and Robotics, Gliwice, Poland

Acknowledgement

This work has been supported by the National Centre of Research and Development funds in the years 2010 - 2012 as development project OR00 0132 12.

8. References

- [1] M. Bao, Micro mechanical transducers: pressure sensors, accelerometers, and gyroscopes, Elsevier, 2000,
- [2] W. Williamson, G. Glenn, V. Dang, J. Speyer, S. Stecko, J. Takacs, Sensor Fusion Applied to Autonomous Aerial Refueling, *Journal of Guidance Control and Dynamics*, Vol. 32, Issue 1, p. 262-275, 2009,
- [3] I. Skog, P. Handel, Calibration of a Mems Inertial Measurement Unit, XVII Imeko World Congress, Metrology for a Sustainable Development, September 17-22, Rio De Janeiro, Brasil, 2006,
- [4] K. H. Kim, J. G. Lee, C. G. Park, Adaptive Two-Stage Extended Kalman Filter for a Fault-Tolerant INS-GPS Loosely Coupled System, *IEEE Transactions On Aerospace And Electronic Systems*, Vol. 45, No. 1, January 2009,
- [5] H. Junker, O. Amft, P. Lukowicz, G. Troster, Gesture spotting with body-worn inertial sensors to detect user activities, *Pattern Recognition* 41, 2010-2024, 2008,
- [6] J. Moreno, E. Rocon De Lima, A. Ruiz, F. Brunetti, J. Pons, Design and implementation of an inertial measurement unit for control of artificial limbs: Application on leg orthoses, *Sensors And Actuators B: Chemical*, Vol. 118, Issues 1-2, p. 333-337, October 2006,
- [7] D. H. Titterton, J. L. Weston, Strapdown Inertial Navigation Technology, London: Peregrinus, Ltd., 1997,
- [8] O. Woodman, R. Harle, Pedestrian localization for indoor environments, *Proceeding UbiComp '08, Proceedings of the 10th International Conference on Ubiquitous computing*, New York, Usa, 2008,
- [9] A. Nawrat, W. Ilewicz, Inertial Navigation using low cost IMU – calculations of UAV orientation in 3-D space, *Technological Advancement in Defence and Security of a State*, p. 45-61, ISBN: 978-83-62652-06-8, 2010,
- [10] A. Nawrat, *Modelling and Control of Unmanned Aerial Vehicles*, ISBN: 978-83-7335-580-4, 2009.